RECEIVED ; ACCEPTED 2004 JUNE 9
Preprint typeset using LaTeX style emulateapj v. 11/12/01

ARE THE JETS ACCELERATED FROM THE DISK CORONAS IN SOME ACTIVE GALACTIC NUCLEI?

XINWU CAO
Shanghai Astronomical Observatory, Chinese Academy of Sciences, 80 Nandan Road, Shanghai, 200030, China
Email: cxw@center.shao.ac.cn
Received ; accepted 2004 June 9

ABSTRACT

We use a sample of radio-loud active galactic nuclei (AGNs) with estimated central black hole masses to explore their jet formation mechanisms. The jet power of AGNs is estimated from their extended radio luminosity. It is found that the jets in several AGNs of this sample are too powerful to be extracted from the standard thin accretion disks or rapidly spinning black holes surrounded by standard thin disks. If the advection dominated accretion flows (ADAFs) are present in these AGNs, their bright optical continuum luminosity cannot be produced by pure-ADAFs due to their low accretion rates and low radiation efficiency, unless the ADAFs transit to standard thin disks at some radii $R_{\rm tr}$. If this is the case, we find that the dimensionless accretion rates $\dot{m}=\dot{M}/\dot{M}_{\rm Edd}$ as high as ≥ 0.05 and transition from ADAFs to standard thin disks at rather small radii around $\sim 20GM_{\rm bh}/c^2$ are required to explain their bright optical continuum emission. We propose that the disk-corona structure is present at least in some AGNs in this sample. The plasmas in the corona are very hot, and the pressure scale-height of the corona $H_{\rm c}\sim R$. Powerful jets with $Q_{\rm jet}\sim L_{\rm bol}$ (bolometric luminosity) can form by the large-scale magnetic fields created by dynamo processes in the disk corona of some AGNs. The maximal jet power extractable from the corona $Q_{\rm jet}^{\rm max}\leq 0.6L_{\rm c}$ ($L_{\rm c}$ is the corona luminosity) is expected by this jet formation scenario. The statistic results on the sample of AGNs are consistent with the predictions of this scenario. Finally, the possibility that the jet is driven from a super-Keplerian rotating hot layer located between the corona and the cold disk is discussed. We find that, in principle, this layer can also produce a powerful jet with $Q_{\rm jet}\sim L_{\rm bol}$.

Subject headings: galaxies: active—galaxies: jets—accretion, accretion disks—black hole physics

1. INTRODUCTION

Relativistic jets have been observed in many radio-loud AGNs and are believed to be formed very close to the black holes. In currently most favored models of the formation of the jet, the power is generated through accretion and then extracted from the disk/black hole rotational energy and converted into the kinetic power of the jet, namely, the Blandford-Payne and Blandford-Znajek mechanisms (Blandford & Payne 1982; Blandford & Znajek 1977). Both these two jet formation mechanisms predict a link between the accretion disk and jet. The disk-jet connection has been investigated by many authors using observational data in different ways (e.g., Rawlings & Saunders 1991; Falcke & Biermann 1995; Xu, Livio, & Baum 1999; Cao & Jiang 1999; 2001), which indicates an intrinsic link between accretion disks and jets. However, this cannot rule out the Blandford-Znajek jet formation mechanism. The magnetic fields are maintained by the currents in the accretion disk surrounding the rapidly spinning black hole, so the power extracted from a rapidly spinning black hole by the Blandford-Znajek mechanism depends on the properties of the disk near the black hole as well.

It's still unclear which mechanism is responsible for jet formation in AGNs. The relative importance of these two jet formation mechanisms is explored by different authors (e.g., Ghosh & Abramowicz 1997; Livio, Ogilivie, & Pringle 1999, hereafter L99; Cao 2002b). Ghosh & Abramowicz (1997) doubted the importance of the Blandford-Znajek process. For a black hole of given mass and angular momentum, the strength of the Blandford-Znajek process depends crucially on the strength of the poloidal field threading the horizon of the hole. The magnetic field threading a hole should be maintained by the currents situated in the inner region of the surrounding accretion disk. They argued that the strength of the field threading a black hole has been overestimated. Livio, Ogilivie, & Pringle (1999) re-investigated the problem and pointed out that even the calculations of Ghosh & Abramowicz (1997) have overestimated the power of the Blandford-Znajek process, since they have overestimated the strength of the large-scale field threading the inner region of an accretion disk, and then the efficiency of the Blandford-Znajek process. The length scale of the fields created by dynamo processes is of the order of the disk thickness $\sim H$. The large-scale field can be produced from the small-scale field created by dynamo processes as $B(\lambda)\propto\lambda^{-1}$ for the idealized case, where λ is the length scale of the field (Tout & Pringle 1996; Romanova et al. 1998). So, the large-scale field is very weak, if the field is created in the thin accretion disks. L99 estimated the maximal jet power extracted from an accretion disk on the assumption that the toroidal field component is of the same order of the poloidal field component at the disk surface. They argued that the maximal jet power extracted from an accretion disk (the Blandford-Payne mechanism) dominates over the maximal power extracted by the Blandford-Znajek process (L99). For the ADAF cases, the disk thickness $H\sim R$ and the jets can be driven by the large-scale magnetic fields created by dynamo processes (e.g., Armitage & Natarajan 1999). The maximal jet power extracted from rotating black holes and ADAFs was calculated by Armitage & Natarajan (1999) and Meier (2001). Instead of the ADAF model, Merloni & Fabian (2002) proposed that the jets in low-luminosity AGNs may be magnetically (or thermally) driven from the coronas above the geometrically thin, optically thin disks accreting at low rates. The gas in the corona is almost virilized, and the thickness of the corona is $\sim R$. The large-scale magnetic fields created by dynamo processes in the corona are significantly stronger than the thin disk due to the fact of the corona thickness being much larger than the cold thin disk, and the disk corona may there-

fore power a stronger jet than the thin disk. In principle, the maximal jet power can be extracted for different jet formation mechanisms can be calculated if the central black hole mass and accretion rate are known.

There are different approaches proposed to measure the black hole masses in AGNs. The tight correlation between central black hole mass $M_{\rm bh}$ and stellar dispersion velocity σ of the host galaxy is used to estimate the black hole mass for the sources with measured stellar dispersion velocity (e.g., Ferrarese & Merritt 2000; Gebhardt et al. 2000). The central black hole mass can also be estimated from its host galaxy luminosity by using the correlation between black hole mass $M_{\rm bh}$ and host galaxy luminosity M_R at R-band (e.g., McLure & Dunlop 2002). However, there are only a small fraction of AGNs with measured stellar dispersion velocity or host galaxy luminosity, which prevents us from using these approaches to estimate the masses of black holes in most AGNs. Kaspi et al. (2000) measured the sizes of broad-line regions (BLRs) in several tens Seyfert 1 galaxies and quasars from the time delay between their variabilities in optical continuum emission and broad-line emission using the reverberation mapping method (Peterson 1993). The central black hole masses of these AGNs have been estimated from their broad-line widths on the assumption that the motion of the clouds in BLR are virilized (Kaspi et al. 2000). They found a correlation between the measured BLR size and optical continuum luminosity for their radio-quiet AGN sample. As only a small fraction of AGNs have measured BLR sizes, this empirical relation between $R_{\rm BLR}$ and optical continuum luminosity λL_λ are employed to estimate the masses of black holes in AGNs from their broad-line widths (e.g., Laor 2000; McLure & Dunlop 2001; Gu, Cao, & Jiang 2001). McLure & Dunlop (2001) compared the virilized Hβ black hole mass estimates with those estimated from $M_{\rm bh}-\sigma$ relation for a sample of radio-loud AGNs. They found that the virilized Hβ black hole masses are systematically lower than that derived from the stellar velocity dispersion, and they concluded that the disk-like BLR geometry may be in these sources. This is in general consistent with the anti-correlation between broad Hβ line width and $R_{\rm c}$ (the ratio of the strengths of the radio core to the lobe) for a flat-spectrum radio-loud AGNs found by Wills & Browne (1986). The inclination angles of the jets in flat-spectrum AGNs are believed to be small with respect to the line of sight, and their optical continuum emission may probably beamed (see Urry & Padovani 1995, and references therein). The black hole mass estimate for flat-spectrum radio-loud AGNs using the broad-line widths and optical continuum luminosities may be lower than their real values, which implies that black hole mass estimated from the broad-line width may be affected by the disk-like BLR orientation (McLure & Dunlop 2001).

In this work, we use a sample of AGNs to explore the jet formation in these AGNs. The black hole masses of the sources in this sample are estimated from their optical continuum luminosities and the widths of broad-line Hβ.

The sample we use in this investigation is radio-selected, which includes some sources with very strong jets. In this work, we will focus on how the powerful jets are formed in the regions near black holes in these sources.

2. BLACK HOLE MASSES AND ACCRETION RATES

Kaspi et al. (2000) derived an empirical relation between the BLR size and optical continuum luminosity

$$R_{\rm BLR} = (32.9^{+2.0}_{-1.9}) \left[\frac{\lambda L_\lambda(5100)}{10^{44}{\rm ergs\ s^{-1}}}\right]^{0.700\pm0.033} {\rm lt-days}, \quad (1)$$

for a sample of Seyfert 1 galaxies and quasars, in which the sizes of BLRs are measured with the reverberation mapping method (Peterson 1993). The central black hole masses $M_{\rm bh}$ can be estimated from the velocities $V_{\rm BLR}$ of the clouds in the BLRs

$$M_{\rm bh} = \frac{V^2_{\rm BLR} R_{\rm BLR}}{G}, \quad (2)$$

where the motions of the clouds are assumed to be virilized and isotropic. The velocities of the clouds in BLRs $V_{\rm BLR}$ are derived from the width of the broad emission lines. For most AGNs, the BLR sizes have not been measured by the reverberation mapping method, the empirical relation (1) is instead used to estimate the BLR sizes. The central black hole masses of AGNs have been estimated from their broad-line widths and optical continuum luminosity (e.g., Laor, 2000; McLure & Dunlop 2001; Gu, Cao, & Jiang 2001). In this work, we use the sample of Gu, Cao, & Jiang (2001). The sources in their sample are selected from a parent sample consisting of 1-Jy, S4, and S5 radio catalogues. As this is a radio-selected sample, it includes most strong radio sources. We assume the physics of BLRs in radio-loud quasars is similar to radio-quiet quasars in the sample of Kaspi et al. (2000), i.e., the tight correlation between the BLR size and optical ionizing luminosity is hold for radio-loud quasars. The central black hole masses of 86 radio-loud (RL) AGNs are estimated by using their broad-line width data and optical continuum luminosities. These 86 AGNs consist of 55 flat-spectrum sources and 31 steep-spectrum sources. We adopt their sample for our present investigation. All the profile data of broad emission line Hβ and derived black hole masses of these sources are listed in Gu, Cao, & Jiang (2001).

For normal bright AGNs, the bolometric luminosity can be estimated from their optical luminosity $L_{\lambda,{\rm opt}}$ at 5100 by (Kaspi et al. 2000)

$$L_{\rm bol} \simeq 9\lambda L_{\lambda,{\rm opt}}, \quad (3)$$

which is only a rough estimate. The coefficient in Eq. (3) may vary for AGNs with different spectral energy distributions.

As the central black hole masses are available for the sources in this sample, we can use Eq. (3) to derive the dimensionless accretion rates $\dot{m}$ of these AGNs. The derived dimensionless accretion rate is given by

$$\dot{m} = \dot{M}/\dot{M}_{\rm Edd} \simeq L_{\rm bol}/L_{\rm Edd}. \quad (4)$$

This is valid for standard thin accretion disks, because the radiative efficiency of thin disks is a constant for given black hole spin parameter a. Combining the relations (1) and (2), we can obtain

$$M_{\rm bh} \propto V^2_{\rm BLR} L^{0.7}_{\lambda,{\rm opt}}. \quad (5)$$

So, using the relations (3), (4), and (5), we get

$$\dot{m} \propto V^{-2}_{\rm BLR} L^{0.3}_{\lambda,{\rm opt}}, \quad (6)$$

since $L_{\rm Edd} \propto M_{\rm bh}$.

It should be cautious for the estimated black hole masses especially for flat-spectrum AGNs, because of not having considered the orientational effects either for the broad-line width or the beamed optical continuum emission. The fact that the virilized Hβ black hole mass estimates are systematically lower than those estimated from $M_{\rm bh}-\sigma$ relation implies that the BLR geometry may be disk-like. The black hole masses estimated for flat-spectrum sources using Hβ line widths may probably

be underestimated (McLure & Dunlop 2001). The errors on the present estimate of the dimensionless accretion rate may be caused by the uncertainties on the black hole mass estimate because of orientational effects, the beamed optical continuum emission, and the coefficient in relation (3). How these uncertainties on the estimates of the black hole mass $M_{\rm bh}$, bolometric luminosity $L_{\rm bol}$, and the dimensionless accretion rate $\dot{m}$ may affect our conclusions will be discussed in Sect. 6.

3. JET POWER

The jet power can be estimated from low-frequency radio luminosity by

$$Q_{\rm jet} \simeq 3\times10^{38} f^{3/2} L_{\rm ext,151}^{6/7}\ {\rm W}, \quad (7)$$

where $L_{\rm ext,151}$ is the extended radio luminosity at 151 MHz in units of 10^{28} W Hz^{-1} sr^{-1} (Willott et al. 1999). Willott et al. (1999) have argued that the normalization is very uncertain and introduced the factor f to account for these uncertainties. They use a wide variety of arguments to suggest that $1 \leq f \leq 20$. In this paper, we conservatively adopt the lower limit $f = 1$. For some flat-spectrum sources, their radio/optical continuum emission is strongly beamed towards us because of their relativistic motions and small viewing angles of the jets with respect to the line of sight. It is found that the spectra of some flat-spectrum quasars are flat even at the wavelength around 151 MHz, which implies that the radio emission from these sources at 151 MHz is still dominated by the core emission rather than the extended emission. So, the observed low-frequency radio emission at 151 MHz may still be Doppler beamed. We therefore use the extended radio emission measured by VLA to estimate the jet power (see Cao 2003). The VLA observations are usually preformed at a frequency much higher than 151 MHz. The extended radio emission measured by the VLA has to be K-corrected to 151 MHz in the rest frame of the source assuming $\alpha_{\rm e} = 0.8$ ($f_\nu \propto \nu^{-\alpha_{\rm e}}$) (Cassaro et al. 1999). Apart from steep-spectrum AGNs, we find 41 flat-spectrum AGNs with extended emission data in this sample.

4. JET FORMATION MECHANISMS

L99 estimated the maximal strength of the large-scale fields driving the jets, and then the maximal jet power extracted from the rapidly spinning black hole or the accretion disk on the assumption of the fields being amplified by dynamo processes. We follow L99, the maximal jet power extracted from a rotating black hole or an accretion disk can be calculated for a standard thin disk, if the black hole mass $M_{\rm bh}$ and accretion rate $\dot{m}$ are specified.

4.1. *Jet power extracted from standard thin disks*

The maximal power of the jet accelerated by an magnetized accretion disk is

$$L_{\rm BP}^{\rm max} = 4\pi \int \frac{B_{\rm pd}^2}{4\pi} R^2 \Omega(R) dR, \quad (8)$$

where $B_{\rm pd} \sim B_\varphi$ is assumed, and $B_{\rm pd}$ is the strength of the large-scale ordered poloidal field at the disk surface.

The strength of the field at the disk surface is usually assumed to scale with the pressure of the disk, as done in Ghosh & Abramowicz (1997). However, L99 pointed out that the large-scale field can be produced from the small-scale field created by dynamo processes as $B(\lambda) \propto \lambda^{-1}$ for the idealized case, where λ is the length scale of the field (Tout & Pringle 1996; Romanova et al. 1998). So, the large-scale field threading the disk is related with the field produced by dynamo processes can be approximated by (L99)

$$B_{\rm pd} \sim \frac{H}{R} B_{\rm dynamo}. \quad (9)$$

The dimensionless pressure scale-height of the disk H/R is given by (Laor & Netzer 1989)

$$\frac{H}{R} = 15.0 \dot{m} r^{-1} c_2, \quad (10)$$

where the coefficient c_2 is defined in Novikov & Thorne (1973, hereafter NT73), and the dimensionless quantities are defined by

$$r = \frac{R}{R_{\rm G}}, \quad R_{\rm G} = \frac{GM_{\rm bh}}{c^2}, \quad \dot{m} = \frac{\dot{M}}{\dot{M}_{\rm Edd}},$$

and

$$\dot{M}_{\rm Edd} = \frac{L_{\rm Edd}}{\eta_{\rm eff} c^2} = 1.39\times10^{15} m\ {\rm kg\ s^{-1}}, \quad m = \frac{M_{\rm bh}}{M_\odot} \quad (11)$$

where $\eta_{\rm eff} = 0.1$ is adopted.

The dimensionless scale-height of the disk H/R is in principle a function of R, and it reaches a maximal value in the inner region of the disk (Laor & Netzer 1989). We adopt the maximal value of H/R in the estimate of large-scale field strength $B_{\rm pd}$ at the disk surface.

As L99, the strength of the magnetic field produced by dynamo processes in the disk is given by

$$\frac{B_{\rm dynamo}^2}{4\pi} \sim \frac{W}{2H}, \quad (12)$$

where W is the integrated shear stress of the disk, and H is the scale-height of the disk. For a relativistic accretion disk, the integrated shear stress is given by Eq. (5.6.14a) in NT73. Equation (12) can be re-written as

$$B_{\rm dynamo} = 3.56\times10^8 r^{-3/4} m^{-1/2} A^{-1} B E^{1/2} {\rm gauss}, \quad (13)$$

where A, B and E are general relativistic correction factors defined in NT73.

In standard accretion disk models, the angular velocity of the matter in the disk is usually very close to Keplerian velocity. For a relativistic accretion disk surrounding a rotating black hole, the Keplerian angular velocity is given by

$$\Omega(r) = 2.034\times10^5 \frac{1}{m(r^{3/2}+a)}\ {\rm s^{-1}}, \quad (14)$$

where a is dimensionless specific angular momentum of a rotating black hole.

We use Eqs. (9)–(14), the maximal power of the jet accelerated from a magnetized disk is available by integrating Eq. (8), if some parameters: m, $\dot{m}$, a, are specified.

As discussed in L99, the power extracted from a rotating black hole by the Blandford-Znajek process is determined by the hole mass m, the spin of the hole a, and the strength of the poloidal field threading the horizon of a rotating hole $B_{\rm ph}$:

$$L_{\rm BZ}^{\rm max} = \frac{1}{32} \omega_{\rm F}^2 B_\perp^2 R_{\rm h}^2 c a^2, \quad (15)$$

for a black hole of mass m and dimensionless angular momentum a, with a magnetic field $B_\perp$ normal to the horizon at $R_{\rm h}$.

Here the factor $\omega_F^2 \equiv \Omega_F(\Omega_h - \Omega_F)/\Omega_h^2$ depends on the angular velocity of field lines Ω_F relative to that of the hole, Ω_h. In order to estimate the maximal power extractable from a spinning black hole, we adopt $\omega_F = 1/2$. As the field $B_\perp$ is maintained by the currents in the accretion disk surrounding the hole, the strength of $B_\perp$ should be of the same order of that in the inner edge of the disk, and $B_\perp \simeq B_{pd}(r_{in})$ is therefore adopted.

4.2. *Jet power extracted from the disk coronas*

In this work, we only consider the case of the jets being magnetically driven by the fields created in the coronas of the disks, as recently suggested by Merloni & Fabian (2002) for the black holes accreting at low rates.

In the disk-corona scenario, the cold disk and the hot corona above the disk are in pressure equilibrium. Most gravitational energy of the accretion matter is released in the hot corona (Haardt & Maraschi 1991; Kusunose, & Mineshige 1994; Svensson, & Zdziarski 1994). A small fraction of the soft photons from the cold disk is Compton up-scattered to X-ray photons by the hot electrons in the corona. Even if the magnetic pressure is in equipartition with the gas pressure, the radiation of the Compton scattering dominates over the synchrotron radiation in the corona (e.g., Liu, Mineshige, & Shibata 2002). Roughly about half of the scattered X-ray photons illuminate the cold disk (Haardt & Maraschi 1991; Nakamura & Osaki 1993; Cao et al. 1998; Kawaguchi, Shimura, & Mineshige 2001). Most soft photons from the disk leave the system without being scattered in the corona, and they are observed as optical/UV continuum. The cold disk in the disk-corona scenario has roughly about half brightness of a standard disk without a corona, if they are accreting at the same rate (Haardt & Maraschi 1991). The gases in the coronas are nearly virilized, their thermal velocity $V_{th} \sim (GM/R)^{1/2}$. Thus, the thickness of the corona $H_c \sim c_s/\Omega_K \sim R$, as the sound speed $V_s \sim V_{th}$ (Nakamura & Osaki 1993). The maximal magnetic stresses created by the dynamo processes are

$$\frac{B_{dyn}^2}{4\pi} \sim \frac{W_c}{2H_c}, \tag{16}$$

where $W_c = 2H_c w_c$ is the integrated shear stress of the corona (Shakura & Sunyaev 1973; Livio, Ogilivie, & Pringle 1999). As the scale-height of the corona $H_c \sim R$, the fields created by the dynamo processes have length scale of R. The maximal jet power can be extracted from the corona in unit surface area is

$$q_j^{max} \sim \frac{B_{dyn}^2}{4\pi} R\Omega_K(R). \tag{17}$$

The viscous dissipation in the corona is

$$f_{vis}^+ = \frac{1}{2} W_c R \left|\frac{d\Omega}{dR}\right| = \frac{3}{4} W_c \Omega_K(R) \tag{18}$$

in unit surface area (Shakura & Sunyaev 1973). Combing Eqs. (16)-(18) and noting $H_c \sim R$ for the corona, we have

$$q_j^{max} \sim \frac{2}{3} f_{vis}^+. \tag{19}$$

Integrating Eq. (19) over the the surface of the corona on the assumption of local equilibrium between the radiation and energy dissipation in the corona, we obtain

$$Q_{jet}^{max} \sim \frac{2}{3} L_c, \tag{20}$$

where L_c is corona luminosity. In the disk-corona scenario, almost all gravitational energy of the accretion matter is released in the corona, i.e., $L_c \simeq L_{bol}$ (Haardt & Maraschi 1991). The emission of the corona is mainly in X-ray bands, half of which leaves the disk-corona system and is observed as X-ray emission and the left half X-ray photons illuminate the cold disk to re-radiate in optical/UV bands (Haardt & Maraschi 1991). Thus, we have

$$L_X \simeq \frac{L_{bol}}{2} \tag{21}$$

and

$$Q_{jet}^{max} \sim \frac{2}{3} L_{bol} \simeq \frac{4}{3} L_X, \tag{22}$$

which indicates that the jets can be more efficiently accelerated from the coronas above the disks than directly from the thin disks (see the discussion on the jet accelerated by the fields of the thin disks in Sect. 1).

5. SPECTRA OF THE DISKS

The ADAF will transit to a standard optically thick, geometrically thin accretion disk at a radius outside R_{tr} (Esin, McClintock, & Narayan 1997). Here, we consider a general case, i.e., an ADAF is present near the black hole and it transits to a cold standard disk (SD) beyond the transition radius R_{tr} (Esin, McClintock, & Narayan 1997).

The flux due to viscous dissipation in the outer region of the disk is

$$F_{vis}(R) \simeq \frac{3GM_{bh}\dot{M}}{8\pi R^3}, \tag{23}$$

which is a good approximation for $R_{tr} \gg R_{in}$. The local disk temperature of the thin cold disk is

$$T_{disk}(R) = \frac{F_{vis}^{1/4}(R)}{\sigma_B^{1/4}}, \tag{24}$$

by assuming local blackbody emission. In order to calculate the disk spectrum, we include an empirical color correction for the disk thermal emission as a function of radius. The correction has the form (Chiang 2002)

$$f_{col}(T_{disk}) = f_\infty - \frac{(f_\infty - 1)[1 + \exp(-\nu_b/\Delta\nu)]}{1 + \exp[(\nu_p - \nu_b)/\Delta\nu]}, \tag{25}$$

where $\nu_p \equiv 2.82 k_B T_{disk}/h$ is the peak frequency of blackbody emission with temperature T_{disk}. This expression for f_{col} goes from unity at low temperatures to f_∞ at high temperatures with a transition at $\nu_b \approx \nu_p$. Chiang (2002) found that $f_\infty = 2.3$ and $\nu_b = \Delta\nu = 5 \times 10^{15}$ Hz can well reproduce the model disk spectra of Hubeny et al. (2001). The disk spectra can therefore be calculated by

$$L_\nu = 8\pi^2 \left(\frac{GM}{c^2}\right)^2 \frac{h\nu^3}{c^2} \int_{r_{tr}}^{\infty} \frac{rdr}{f_{col}^4[\exp(h\nu/f_{col}k_B T_{disk}) - 1]}. \tag{26}$$

In this ADAF+SD scenario, the ionizing luminosity from the disk is a combination of the emission from the inner ADAF and outer standard disk regions. Cao (2002a)'s calculations indicate that the optical continuum emission from the inner ADAF region can be neglected compared with that from outer SD region if R_{tr} is around tens to several hundreds Schwarschild radii, which is due to low radiation efficiency of ADAFs.

6. RESULTS

In Fig. 1, we plot the relation between $L_{\rm bol}/L_{\rm Edd}$ and $Q_{\rm jet}/L_{\rm bol}$. The jet power of AGNs is estimated from the low-frequency extended radio luminosity by using relation (7). The maximal jet power can be extracted by the magnetic fields created in the standard accretion disks (solid line) and the rapidly spinning black holes of $a = 0.95$ (dotted line) are calculated by using the method described in Sect. 4.1. The flat-spectrum and steep-spectrum sources are labelled as squares and circles respectively. The sources above the solid line in Fig. 1 are labelled as filled square(circles) (hereafter these sources are referred as high-jet-power sources). This indicates that the Blandford-Payne mechanism is unable to produce sufficient jet power observed in the high-jet-power sources, if only standard thin accretion disks are present in these sources. The jets in almost all sources of this sample cannot be powered only by the Blandford-Znajek mechanism, even if the black holes in these sources are rapidly spinning at $a = 0.95$.

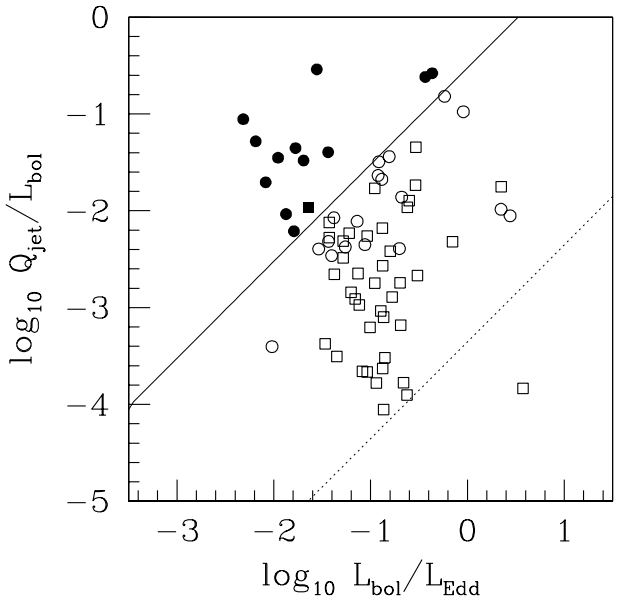

FIG. 1.— The ratio $L_{\rm bol}/L_{\rm Edd}$ versus the ratio $Q_{\rm jet}/L_{\rm bol}$. The squares represent flat-spectrum sources, and the circles are for steep-spectrum sources. The solid line represents the maximal jet power extracted from a standard thin accretion disk (the Blandford-Payne mechanism), while the dotted line represents the maximal jet power extracted from a rapidly spinning black hole $a = 0.95$ surrounded by a standard thin accretion disk (the Blandford-Znajek mechanism). The sources above the solid line, referred as high-jet-power sources, are labelled as filled circles(square).

As mentioned in Sect. 2, there are uncertainties on the estimates of the black hole mass $M_{\rm bh}$, bolometric luminosity $L_{\rm bol}$, and then the dimensionless accretion rate $\dot{m}$. The beamed optical continuum emission from the jets may lead to overestimate of bolometric luminosity $L_{\rm bol}$ especially for flat-spectrum sources, which would shift the real locations of the sources in Fig. 1 towards the direction away from the line (solid) representing the maximal jet power extracted by the Blandford-Payne mechanism (see Fig. 1). If the disk-like BLR geometry is present in these sources, their black hole masses may be underestimated (McLure & Dunlop 2001) and the real locations of the sources should also be shifted towards the direction away from the maximal jet power line in Fig. 1. The uncertainty on the coefficient in relation (3) can also lead to errors on the estimate of bolometric luminosity $L_{\rm bol}$. If the present coefficient in relation (3) is overestimated, the locations of high-jet-power sources will be also shifted towards the direction away from the maximal jet power line. The jets in all these high-jet-power sources can be extracted by the Blandford-Payne mechanisms for thin disk cases, only if the coefficient in relation (3) is significantly underestimated at more than one order of magnitude, i.e., > 100 is required instead of 9 in relation (3). So, the conclusion that the jets in these high-jet-power sources cannot be accelerated by the Blandford-Payne mechanism for standard thin disk cases will not be altered by the uncertainties of the estimates on the black hole mass $M_{\rm bh}$, bolometric luminosity $L_{\rm bol}$, or dimensionless accretion rate $\dot{m}$, unless the present coefficient in relation (3) is underestimated at an order of magnitude, which seems impossible.

The relation between black hole mass $M_{\rm bh}$ and optical continuum luminosity L_λ at 5100 is plotted in Fig. 2. The optical continuum emission from a pure ADAF can be calculated by using the approach proposed by Mahadevan (1997). We use the same approach proposed by Cao (2002a) to calculate the maximal optical continuum emission from an ADAF as a function of black hole mass $M_{\rm bh}$. The maximal optical continuum emission requires the parameter $\beta = 0.5$, which describes the magnetic field strength with respect to gas pressure, and viscosity $\alpha = 1$. Changing the value of accretion rate $\dot{m}$, we can find the maximal optical continuum luminosity for given black hole mass (see Cao, 2002a for details). It is found that all sources have optical continuum luminosity higher than the maximal optical luminosity expected from pure ADAFs, which implies that the emission from pure-ADAFs is unable to explain the optical ionizing luminosity of these sources. We then consider another possibility, i.e., the ADAF transits to a standard thin disk outside the transition radius $R_{\rm tr}$. The theoretical calculations of the optical continuum luminosity for such ADAF+SD systems with different accretion rates and transition radii are also plotted in the figure (the calculations are carried out as described in Sect. 5). It is found that ADAFs may be present in the inner region of the disk in these high-jet-power sources only if the critical accretion rates $\dot{m}_{\rm crit}$ are as high as $\geq$0.05. For flat-spectrum sources, the optical continuum emission from the accretion disks may be overestimated and the accretion rates inferred from Fig. 2 may be larger than their real values. The beaming effect is believed to be unimportant for steep-spectrum sources because of their relatively larger angles than flat-spectrum sources with respect to the line of sight, and it is therefore suggested that the optical continuum emission of steep-spectrum sources is mainly from their accretion disks (Serjeant et al. 1998). The high-jet-power sources in this sample are steep-spectrum sources except one flat-spectrum source. So, the estimated dimensionless accretion rates for these high-jet-power sources should be less affected by the beamed jet emission than flat-spectrum sources, and the main results on the accretion rates and transition radii for these high-jet-power sources should not be changed significantly.

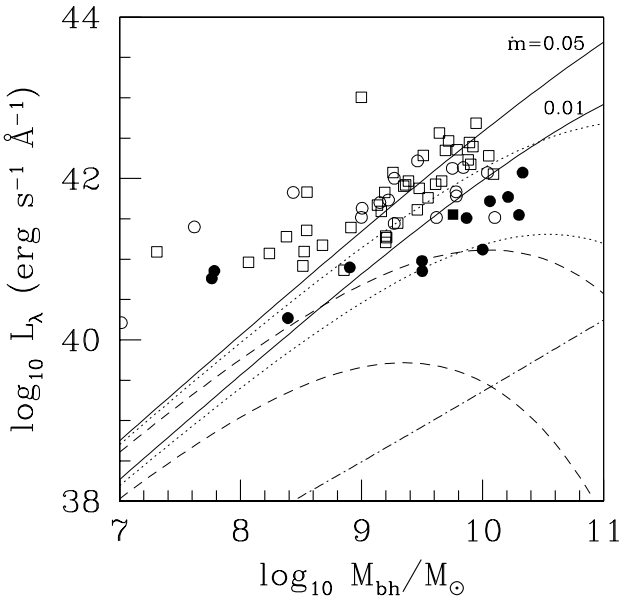

FIG. 2.— The black hole mass $M_{\rm bh}$ versus optical luminosity L_λ at 5100 Å. The dash-dotted line represents the maximal optical continuum luminosity from pure-ADAFs. The solid lines represent standard disks accreting at $\dot{m}$ = 0.01 and 0.05, respectively. The dotted and dashed lines represent the ADAF+SD models with different transition radii $R_{\rm tr} = 20GM/c^2$ and $50GM/c^2$, respectively. The upper lines are plotted for $\dot{m}$ = 0.05, while the lower lines are for $\dot{m}$ = 0.01. The symbols are same as Fig. 1.

The relation between bolometric luminosity $L_{\rm bol}$ and jet power $Q_{\rm jet}$ is plotted in Fig. 3. The jet power is lower than the bolometric luminosity for all sources in this sample, which would still hold even if the bolometric luminosity is overestimated by less than an order of magnitude for flat-spectrum sources.

In order to test relation (22) between $Q_{\rm jet}^{\rm max}$ and total X-ray luminosity $L_{\rm X}$ from the disk coronas predicted by the scenario of the jets being magnetically accelerated by the fields created in the disk coronas, we roughly convert X-ray luminosity in $0.1-2.4$ keV $L_{\rm X,0.1-2.4keV}$ detected by ROSAT (Voges et al. 1999) to the total X-ray luminosity assuming the X-ray continuum emission to be in the range from $0.01-100$ keV with a mean energy spectral index $\alpha_{\rm X} = 1$ ($f_{\rm X} \propto E^{-\alpha_{\rm X}}$). This is consistent with the general features of the theoretical calculations on the X-ray spectra from the disk coronas (e.g., Nakamura & Osaki 1993). In this case, the total X-ray luminosity $L_{\rm X} \simeq 2.9 L_{\rm X,0.1-2.4keV}$. In Fig. 4, the relation between K-corrected core radio luminosity $L_{\rm c,5G}$ and X-ray luminosity $L_{\rm X}$. The linear regression considering errors in both coordinates gives (Press et al. 1992)

$$\log_{10} L_{\rm X} = 0.866 \log_{10} L_{\rm c,5G} + 7.517 \qquad (27)$$

for 40 flat-spectrum sources (the solid line in Fig. 4), and

$$\log_{10} L_{\rm X} = 0.371 \log_{10} L_{\rm c,5G} + 29.272 \qquad (28)$$

for 18 steep-spectrum sources (the dotted line in Fig. 4). The Spearmann correlation analyses (Press et al. 1992) show that the correlation for flat-spectrum sources is at the significant level of 99.98 per cent, while it becomes 98.5 per cent for steep-spectrum sources. The different slopes of the correlations between $L_{\rm X}$ and $L_{\rm c,5G}$ for steep-spectrum and flat-spectrum sources are obvious, which may imply that the observed X-ray emission from these two kinds of AGNs may have different origins.

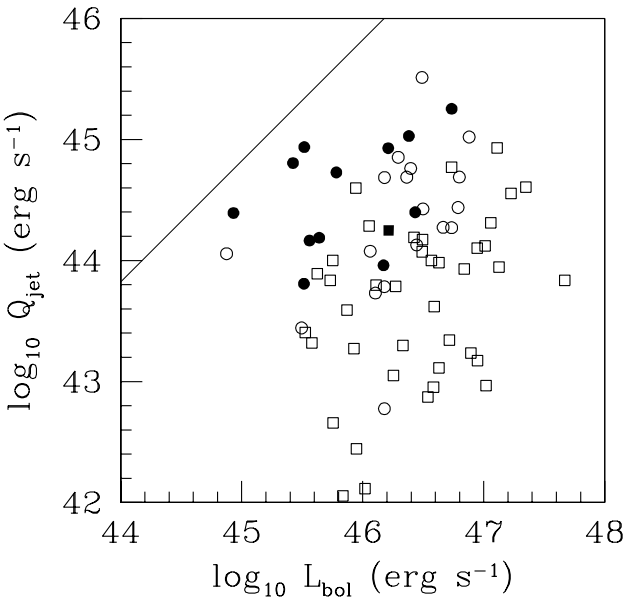

FIG. 3.— The relation between bolometric luminosity $L_{\rm bol}$ and jet power $Q_{\rm jet}$. The line represents $Q_{\rm jet} = 2/3\, L_{\rm bol}$. The symbols are same as Fig. 1.

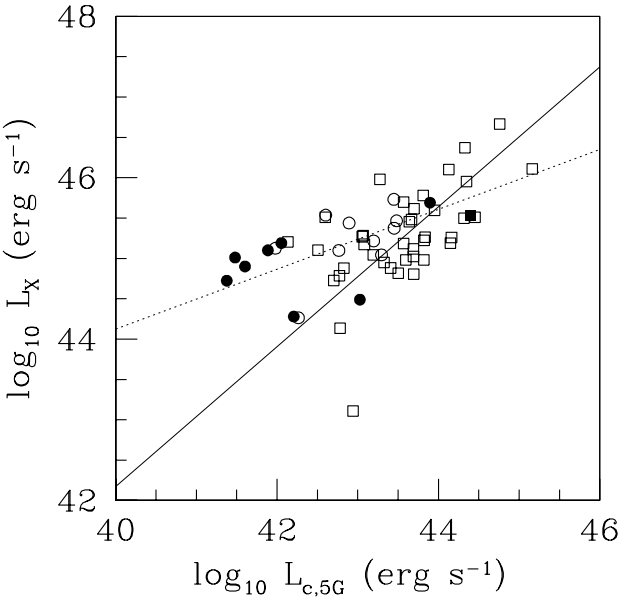

FIG. 4.— The relation between X-ray luminosity $L_{\rm X}$ and core radio luminosity $L_{\rm c}$ at 5 GHz. The solid and dotted lines represent the linear regressions for flat-spectrum and steep-spectrum sources respectively. The symbols are same as Fig. 1.

We plot the relation between X-ray luminosity L_X and jet power Q_{jet} in Fig. 5. We find that almost all sources have $Q_{jet} < L_X$, except one steep-spectrum source with $Q_{jet} \sim L_X$.

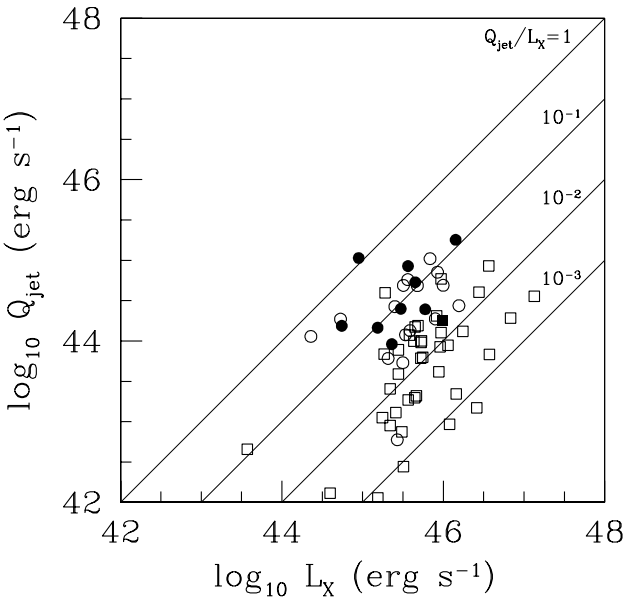

FIG. 5.— The relation between X-ray luminosity L_X and jet power Q_{jet}. The lines represent $Q_{jet}/L_X = 10^{-3}$, 10^{-2}, 10^{-1}, and 1, respectively. The symbols are same as Fig. 1.

7. DISCUSSION

There are 13 sources with jet power above the maximal jet power expected to be extracted from standard thin disks (see Fig. 1), i.e., the fields of thin disks are unable to drive such strong jets in these high-jet-power sources. The jet can be accelerated from an ADAF more efficiently than a standard thin disk, though an accurate calculation on the maximal jet power extracted from an ADAF is still unavailable (Meier 2001). Meier (2001) pointed out that general relativistic effects may be important and a rough estimate of jet power shows that the maximal jet power extracted from an ADAF as high as 10^{45-46} erg s^{-1} may be possible for a rapidly spinning massive black hole ($\sim 10^9 M_\odot$). If ADAFs are present in these sources, they will have fainter optical continuum emission than standard disks due to the lower accretion rates and lower radiation efficiency of ADAFs. It is found that pure-ADAFs are unable to produce observed bright optical continuum luminosity for all sources in this sample (see Fig. 2). However, this cannot rule out the presence of ADAFs in these sources, because the ADAF may transit to a standard thin disk in the region outside the transition radius R_{tr}. In this case, the standard thin disk in the outer region may be responsible for the observed optical continuum emission. The ADAF+SD (standard disk) scenario is tested against observational optical continuum luminosity in Fig. 2. As 12 of 13 high-jet-power sources are steep-spectrum AGNs, the optical continuum emission is believed to be mainly from the accretion disks (Serjeant et al. 1998). It is found that relatively high accretion rates $\dot{m} \geq 0.05$ are required to explain the optical continuum luminosity of these high-jet-power sources, if the ADAFs are truncated at rather small radii (e.g., ≤ 20 Schwarschild radii). If the transition radii are larger than this value, even higher accretion rates are required. The exact value of the critical accretion rate $\dot{m}_{crit}$ is still unclear for an ADAF, which depends on the value of the disk viscosity parameter α, i.e., $\dot{m}_{crit} \simeq 0.28\alpha^2$ (Mahadevan 1997). Recent three-dimensional MHD simulations suggest that the viscosity α in the discs to be ~ 0.1 (Armitage 1998), or $\sim 0.05-0.2$ (Hawley & Balbus 2002). If a value $\alpha = 0.2$ is conservatively adopted, the accretion rates $\dot{m} \leq \dot{m}_{crit} \sim 0.01$ are required for ADAFs. This may probably imply that ADAFs are not present in these high-jet-power sources.

For an ADAF, its bolometric luminosity can be significantly lower than the jet power extracted from the ADAF or the rapidly spinning black hole surrounded by the ADAF, because the radiation efficiency of ADAFs is much lower than the efficiency of power channelled into the jet (Armitage & Natarajan 1999; Meier 2001). We have not found any source in our sample with $Q_{jet} > L_{bol}$ (see Fig. 3). It implies that standard thin disks, at least in the outer regions of the disks, are required to produce observed bright bolometric luminosity, even if ADAFs are present in these sources in the case of $\alpha > 0.2$, though it seems inconsistent with MHD simulations (Hawley & Balbus 2002).

The ADAF solutions may be modified to adiabatic inflow-outflow solutions (ADIOSs), if a powerful wind is present to carry away mass, angular momentum and energy from the accreting gas (Blandford & Begelman 1999). In this case, the accretion rate of the disk is a function of radius r instead of a constant accretion rate along r for a pure ADAF. For an ADIOS flow, the gas swallowed by the black hole is only a small fraction of the rate at which it is supplied, as most of the gas is carried away in the wind before it reaches the black hole. The ADIOS flow has similar local structure as the ADAF accreting at the same rate, so the accretion rate $\dot{m}$ for an ADIOS flow at any radius should be smaller than the critical rate $\dot{m}_{crit}$ of ADAFs. The ADIOS flow is fainter than an ADAF, if they are accreting at the same rate at the outer radius, because the accretion rate of an ADIOS flow decreases while the gas is flowing onto the hole (e.g., Quataert & Narayan (1999); Chang, Choi & Yi (2002)). So, even if an ADIOS flow is present instead of an ADAF in the inner region of the disk, the optical continuum emission is still dominated by the emission from the standard thin disk in the outer region, as the ADAF case (Cao 2002a). Our present spectral analysis for ADAF+SD system are valid even for ADIOS+SD systems. For convection dominated accretion flows (CDAFs), most of the gas circulates in convection eddies rather than accreting onto the black hole (Narayan, Igumenshchev, & Abramowicz 2000; Quataert & Gruzinov 2000). The accretion rates of CDAFs are much smaller than non-convecting ADAFs, and CDAFs are very faint (Ball, Narayan & Quataert 2001). This implies that the accretion rate in a standard thin disk surrounding a CDAF should be much smaller than the critical accretion rate $\dot{m}_{crit}$ in ADAFs, if a steady accretion flow is assumed. The observed bright optical continuum emission in these high-jet-power sources requires the black holes accreting at rather high rates, which seems to rule out the possibility of CDAFs surrounded by standard thin disks in these high-jet-power sources.

The powerful jets in these high-jet-power sources may be accelerated from ADAFs (or ADIOS flows) surrounded by standard thin disks outside ~ 20 Schwarzschild radii accreting at $\dot{m} \geq 0.05$, which is required by observed bright optical contin-

uum emission in these sources. However, such high accretion rates require a high viscosity α, which seems inconsistent with MHD simulations (Hawley & Balbus 2002). Here, we propose an alternative explanation, i.e., the jets, at least in these high-jet-power sources, are accelerated from the coronas of the disks. In this case, the maximal power of the jet accelerated from the corona of the disk can be as high as its bolometric luminosity (see Eq. (22) and Fig. 3), and the strong jets in these high-jet-power sources can be naturally explained by this scenario. The cold disk irradiated by the corona above can produce bright optical continuum emission as observed in these high-jet-power sources.

It should be cautious that the calculations carried out in Sect. 4.2 are on the assumption of a perfect parallel corona structure. The real corona above the cold disk may not always have perfect parallel structure. The time variations and spatial inhomogeneity can be caused by the magnetic fields (e.g., Kawaguchi et al. 2000). So, the maximal jet power extractable from the corona may be lower than that estimated by Eq. (22) because of the inhomogeneous corona structure. Most high-jet-power sources in our sample have $Q_{\rm jet}/L_{\rm bol} \leq 0.1$, while three sources have Qjet$/L_{\rm bol} \simeq 0.3$ (see Fig. 1). The disk-corona scenario may still be a reasonable explanation for jet formation in these high-jet-power sources.

The emission from the coronas is mainly in X-ray bands, and this scenario predicts a relation between the maximal power of the jet accelerated from the corona and X-ray luminosity of the corona (Eq. 22). This prediction can be tested against observations. However, the difficulty arises from the fact that the observed X-ray emission from these radio-loud AGNs may be a mixture of the emission from the jets and accretion disk coronas. If the X-ray emission from the jets in radio-loud AGNs dominates over that from the disk coronas, a correlation between radio core emission and X-ray emission is expected, because both of them are from the jets and Doppler beamed. Figure 4 gives different correlations between core radio luminosity $L_{\rm c,5G}$ and X-ray luminosity $L_{\rm X}$ for flat-spectrum and steep-spectrum AGNs. Falcke, Koerding, & Markoff (2004) used LINERs, FR I galaxies, and BL Lac objects in their investigations on the radio-X-ray correlation, in which ADAFs are believed to be present and the radio and X-ray emission are believed to be dominated by the emission from the jets. The correlation found in this work between radio and X-ray luminosities for flat-spectrum sources is roughly consistent with the correlation given by Falcke, Koerding, & Markoff (2004). The core dominance parameter $R_{\rm c}$ varies over several orders of magnitude for the sources in this sample (Cao & Jiang 2001), which reflects the Doppler factors spread over a large range for these sources. In this work, we do not intend to explore this correlation in detail as done by Falcke, Koerding, & Markoff (2004), because of unknown Doppler beaming factors of the sources in this sample. Nevertheless, the different slopes of the correlations for flat-spectrum and steep-spectrum sources do indicate the different origins of the X-ray emission to be in these two kinds of sources. Compared with flat-spectrum sources, most steep-spectrum sources have brighter X-ray emission than their flat-spectrum counterparts with similar radio core emission (see Fig. 4). This may imply that the X-ray emission from the disk coronas rather than the jets is dominant for steep-spectrum AGNs. If this is the case, the observed X-ray emission from steep-spectrum sources is probably from the disk coronas. We can tentatively use Fig. 5 to test our estimate on the relation between $Q_{\rm jet}^{\rm max}$ and $L_{\rm X}$ (Eq. (22)) expected for the jets magnetically accelerated from the coronas of the disks. It is found in Fig. 5 that $Q_{\rm jet} < L_{\rm X}$ is satisfied for almost all sources except one with $Q_{\rm jet} \sim L_{\rm X}$, which is consistent with the scenario of the jets being magnetically accelerated from the disk coronas. If this scenario is correct, it implies that the factor f in Eq. (7) describing the uncertainty of the jet power estimated from the extended radio luminosity should be close to unit at least for these high-jet-power sources (see Figs. 3 and 5).

Recently, Hujeirat, Camenzind, & Livio (2002) proposed that the jet is launched from a layer, governed by a highly diffusive, super-Keplerian rotating and thermally dominated by virilhot and magnetized ion-plasma. This layer is located between the accretion disk and the corona surrounding the nucleus. In this model, most of the accretion energy can be converted into magnetic and kinetic energies that go into powering the jet (Hujeirat et al. 2003; Hujeirat 2004), and the powerful jet with $Q_{\rm jet} \sim L_{\rm bol}$ can form naturally in such a layer. This model, in principle, can explain the powerful jets of the high-jet-power sources in our present sample, though the detailed numerical model calculations for the jets in these sources are beyond the scope of this paper.

This work is supported by the National Science Fund for Distinguished Young Scholars (grant 10325314), NSFC (grants 10173016; 10333020), and the NKBRSF (grant G1999075403). This research has made use of the NASA/IPAC Extragalactic Database (NED), which is operated by the Jet Propulsion Laboratory, California Institute of Technology, under contract with the National Aeronautic and Space Administration.

REFERENCES

Armitage P.J., 1998, ApJ, 501, L189
Armitage P.J., & Natarajan P., 1999, ApJ, 523, L7
Ball, G. H., Narayan, R., Quataert, E., 2001, ApJ, 552, 221
Blandford R.D., & Begelman M.C., 1999, MNRAS, 303, L1
Blandford R. D., & Payne D. G., 1982, MNRAS, 199, 883
Blandford, R. D., & Znajek, R. L., 1977, MNRAS, 179, 433
Cao, X., 2002a, ApJ, 570, L13
Cao, X., 2002b, MNRAS, 332, 999
Cao, X., 2003, ApJ, 599, 147
Cao, X., Jiang, D.R., 1999, MNRAS, 307, 802
Cao, X., Jiang, D.R., 2001, MNRAS, 320, 347
Cao, X., Jiang, D.R., You, J.H., Zhao, J.L., 1998, A&A, 330, 464
Cassaro, P., Stanghellini, C., Bondi, M., Dallacasa, D., della Ceca, R., & Zappalíd', R. A., A&AS, 139, 601
Chang H.Y., Choi C.S., & Yi I., 2002, AJ, 124, 1948
Chiang, J., 2002, ApJ, 572, 79
Esin, A. A., McClintock, J. E., & Narayan, R., 1997, ApJ, 489, 865
Falcke, H., & Biermann, P.L., 1995, A&A, 293, 665
Falcke, H., Körding, E., & Markoff, S., 2004, A&A, 414, 895
Ferrarese, L., & Merritt, D., 2000, ApJ, 539, L9
Gebhardt, K. et al., 2000, ApJ, 539, L13
Ghosh P., & Abramowicz M. A., 1997, MNRAS, 292, 887
Gu, M., Cao, X., & Jiang, D.R., 2001, MNRAS, 327, 1111
Haardt, F., & Maraschi, L., 1991, ApJ, 380, L51
Hawley, J.F., Balbus, S.A., 2002, ApJ, 573, 738
Hubeny, I., Blaes, O., & Krolik, J. H., Agol, E., ApJ, 559, 680
Hujeirat, A., 2004, A&A, 416, 423
Hujeirat, A., Camenzind, M., & Livio, M., 2002, A&A, 394, L9
Hujeirat, A., Livio, M., Camenzind, M., & Burkert, A., 2003, A&A, 408, 415
Kaspi S., Smith P.S., Netzer H., Maoz D., Jannuzi B.T., & Giveon U., 2000, ApJ, 533, 631
Kawaguchi, T., Mineshige, S., Machida, M., Matsumoto, R., Shibata, K., 2000, PASJ, 52, L1

Kawaguchi, T., Shimura, T., Mineshige, S., 2001, ApJ, 546. 966
Kusunose, M., & Mineshige, S., 1994, ApJ, 423, 600
Laor, A., 2000, ApJ, 543, L111
Laor A., & Netzer H., 1989, MNRAS, 238, 897
Liu, B.F., Mineshige, S., & Shibata, K., 2002, ApJ, 572, L173
Livio M., Ogilivie G. I., & Pringle J. E., 1999, ApJ, 512, 100(L99)
Mahadevan, R., 1997, ApJ, 477, 585
McLure, R. J., & Dunlop, J. S., 2001, MNRAS, 327, 199
McLure, R.J., & Dunlop, J.S., 2002, MNRAS. 331, 795
Meier, D. L., 2001, ApJ, 548, L9
Merloni, A., Fabian, A. C., 2002, MNRAS, 332, 165
Merloni, A., Heinz, S., & Di Matteo, T., 2003, MNRAS, 345, 1057
Nakamura, K., & Osaki, Y., 1993, PASJ, 45, 775
Narayan, R., Igumenshchev, I.V., & Abramowicz, M.A., 2000, ApJ, 539, 798
Novikov I., & Throne K. S., 1973, in Black holes, eds de Witt C. and de Witt B., Gordon & Breach, New York(NT73)
Peterson, B. M., 1993, PASP, 105, 247
Press, W.H., Teukolsky, S.A., Vetterling W.T., & Flannery B.P., 1992, Numerical recipes in FORTRAN: the art of Scientific computing, Cambridge university press.
Quataert, E., & Gruzinov, A., 2000, ApJ, 539, 809
Quataert, E., & Narayan, R., 1999, ApJ, 520, 298
Rawlings S., & Saunders R., 1991, Nature, 349, 138
Romanova M. M., Ustyugova G. V., Koldoba A. V., Chechetkin V. M., & Lovelace R. V. E., 1998, ApJ, 500, 703
Serjeant, S., Rawlings, S., Lacy, M., Maddox, S. J., Baker, J. C., Clements, D., Lilje, P. B., 1998, MNRAS, 294, 494
Shakura, N. I., & Sunyaev, R. A., 1973, A&A, 24, 337
Svensson, R., & Zdziarski, A., 1994, ApJ, 436, 599
Tout C. A., & Pringle J. E., 1996, MNRAS, 281, 219
Urry, C.M., & Padovani, P., 1995, PASP, 107, 803
Voges, W. et al., 1999, A&A, 349, 389
Willott, C.J., Rawlings S., Blundell K.M., & Lacy M., 1999, MNRAS. 309. 1017
Wills, B.J., & Browne, I.W.A., 1986, ApJ, 302, 56
Xu, C., Livio, M., Baum, S., 1999, AJ, 1999, AJ, 118, 1169